Macromolecular Research

Article

DOI 10.1007/s13233-018-6035-y

www.springer.com/13233 pISSN 1598-5032 eISSN 2092-7673

Protein-Patterning on Functionalized, Non-Biofouling Poly[*N*-acryloxysuccinimide-*co*-oligo(ethylene glycol) methyl ether methacrylate] Film-Coated PET Surfaces

Gyeongyeop Han[1]
Yoonyoung Kim[2]
Kyungtae Kang[2]
Bong Soo Lee*[,3]
Jungkyu K. Lee*[,1]

[1] Department of Chemistry and Green-Nano Materials Research Center, Kyungpook National University, Daegu 41566, Korea
[2] Department of Applied Chemistry, Kyung Hee University, Gyeonggi 17104, Korea
[3] Center for Cell-Encapsulation Research, Department of Chemistry, Korea Advanced Institute of Science and Technology (KAIST), Daejeon 34141, Korea

Received July 25, 2017 / Revised November 8, 2017 / Accepted November 18, 2017

Abstract: We successfully fabricated poly(ethylene terephthalate) (PET) surfaces through a perfluoroaryl azide-based photochemical reaction, and subsequently formed an intrinsically activated, non-biofouling poly[*N*-acryloxysuccinimide-*co*-oligo(ethylene glycol) methyl ether methacrylate] on the surface through surface-initiated, controlled radical polymerization. The grafted copolymer film on PET facilely generated a protein pattern using a microcontact printing technique without employing both an activation step to introduce an active functional group (*e.g.,* succinimidyl ester) and a passivation process for minimizing non-specific adsorption. Consequently, we characterized the functionalized PET surfaces by using various methods including contact angle measurement, X-ray photoelectron spectroscopy (XPS), scanning probe microscopy (SPM), field-emission scanning electron microscopy (FE-SEM). In addition, we evaluated the non-biofouling efficacy of the protein-patterned copolymer film on PET by confocal laser scanning microscopy.

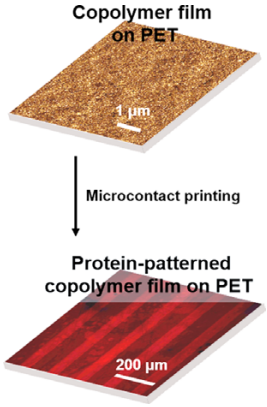

Keywords: organic polymer substrate, copolymer coating, biopatterning, surface-initiated controlled radical polymerization, photochemical reaction.

1. Introduction

Poly(ethylene terephthalate) (PET) has been commonly used as a type of thermoplastic polyester in domains such as food and textile industry, and electrical devices due to its high transparency, low weight, good thermal and UV resistance, economic feasibility, toughness, high stress crack resistance, and excellent processability and moldability.[1-4] In particular, these unique characteristics, for example, make it desirable for applications requiring reliable performances such as electrical encapsulation, photovoltaic panels, and energy components.[5-7] In addition, PET has received attention as a synthetic material for implantable medical devices.[8-10] Thus, it has been utilized for fabrication of surgical mesh, sewing cuffs for heart valves, vascular grafts, prosthesis, shunt, and sutures.[11,12] However, improving the biocompatibility of PET is still a critical issue if it is to be used for human implantation.[13-16] For example, PET fabrics and fibers used as synthetic ligaments have caused severe inflammation in the operated knee joint mainly because of the nonspecific adsorption of biological entities (*e.g.,* protein, cell, and bacteria) on the surface resulting in undesirable biological responses such as host responses.[17,18]

Recently, minimizing biofouling on inorganic substrates such as Si/SiO_2 and gold has been actively investigated by introducing a non-biofouling polymer film on these substrates using immobilization of an initiator, followed by surface-initiated controlled radical polymerization (SI-CRP).[19-22] However, few studies have been conducted on the use of organic polymer substrates due to the limited synthetic methodology for chemically functionalizing the plastic surfaces.[23-25] These limits are mainly result of a lack of chemically functional groups on these surfaces and certain undesirable chemicals effects on plastics. In this respect, the developing synthetic methods applicable to functionalizable plastics play an important role, and we have previously attempted a photochemical immobilization of perfluoroaryl azides on a cyclic olefin copolymer (COC) substrate, consisting of saturated hydrocarbons.[26-28] This strategy employed a simple fabrication and pattern generation, and provided a strong covalent bond of perfluoroaryl azide compounds with the surface when compared with conventional approaches such as chemical oxidation[29,30] and physical graft-

Acknowledgments: This work was supported by Dong-il Culture and Scholarship Foundation research grants to J.K.L. and Basic Science Research Program through the National Research Foundation of Korea (NRF) grant funded by the Ministry of Education (NRF-2017R1D1A1B 03027858) to B.S.L.

***Corresponding Authors:** Bong Soo Lee (leebongsoo@kaist.ac.kr), Jungkyu K. Lee (jkl@knu.ac.kr)

ing.[31] Moreover, we successfully demonstrated a non-biofouling performance of biotin-terminated copolymer films on gold surfaces without employing the passivation and activation processes.[32] On the other hand, we wondered whether our approaches could be applied to versatile organic polymer substrates. Therefore, we demonstrate a functionalized, non-biofouling polymer-coated PET surface using the photochemical reaction with an initiator terminated-perfluoroaryl azide compound, and subsequently with SI-CRP. In addition, we adopt a copolymer system, consisting of two different monomers, where oligo(ethylene glycol) methyl ether methacrylate is used as a non-biofouling material, and *N*-acryloxysuccinimide is employed as a reactive compound bearing a highly reactive functional group (*i.e.,* succinimidyl ester).[32] This copolymer system is envisioned to replace old-fashioned processes (*i.e.,* activation and passivation) after polymerization on the PET surface.

2. Experimental

2.1. Materials

Poly(ethylene terephthalate) (PET, KIMOTO Co., Ltd., Japan), *N*-acryloxysuccinimide (NAS, ≥90%, TCI), oligo(ethylene glycol) methyl ether methacrylate (OEGMEMA, M_n∼300, Aldrich), copper(II) bromide ($CuBr_2$, 99.999%, Aldrich), 2,2'-bipyridyl (≥99%, Aldrich), phosphate buffered saline (PBS, pH 7.4, 10 mM, Aldrich), L-ascorbic acid (≥99%, Aldrich), (+)-biotinyl-3,6,9-trioxaundecanediamine (biotin-TEG-NH_2, Thermo Fisher Scientific), rhodamine-conjugated streptavidin (lyophilized powder from protein in buffered saline solution, Thermo Fisher Scientific), dimethyl sulfoxide (DMSO, ≥99.5%, Aldrich), and nitromethane (99.9+%, Aldrich) were purchased and used without further purification. 2-(2-(2-(4-azido-2,3,5,6-tetrafluorobenzamido)ethoxy)ethoxy)ethyl 2-bromo-2-methylpropanoate (initiator-terminated perfluoroaryl azide) was synthesized by our reported method.[26] Deionized water (pure water, 18.3 MΩ·cm) from the Human Ultra Pure System (Human Corp. South Korea) was used.

2.2. Preparation of initiator-anchored PET surfaces

Bare PET substrates were sonicated with ethanol for 1 min and then dried in a stream of argon. The washed substrates were oxidized using an oxygen-plasma cleaner (Harrick PDC-002) for 1 min at medium strength. Following this, the oxidized substrates were coated with the initiator-terminated perfluoroaryl azide (0.5% w/v in nitromethane) using a spin-coater for 30 s at 2,000 rpm. The resulting substrates were baked in an oven at 60 °C for 20 min, and irradiated with UV light (254 nm, Emerson Electric Co.) for 1 h.[33] The UV-exposed substrates were then washed with nitromethane to remove the physically adsorbed perfluoroaryl azide and dried in a stream of argon, producing the initiator-immobilized PET substrates.

2.3. Formation of biotinylated-copolymer film on PET surfaces

We employed *N*-acryloxysuccinimide (NAS) and oligo(ethylene glycol) methyl ether methacrylate (OEGMEMA) to synthesize an activation-free, bioactive poly(NAS-*co*-OEGMEMA) film. Two different stock solutions were initially prepared (stock solution I: 2 mM $CuBr_2$ and 4 mM 2,2'-bipyridyl in pure water, and stock solution II: 20 mM ascorbic acid in pure water). 50 μL of stock solution I and 50 μL of stock solution II were added into a conical tube, containing NAS (33.8 mg, 0.2 mmol), OEGMEMA (228 μL, 0.8 mmol), pure water (56 μL), and DMSO (626 μL). The resulting pale-brown solution was vigorously stirred for 10 min, and surface-initiated, activators regenerated by electron transfer atom transfer radical polymerization (SI-ARGET ATRP) was initiated by transferring the mixture solution to the tube with the initiator-anchored substrate. After a reaction time of 2 h at room temperature, the polymerization was terminated by removing the substrate. The poly(NAS-*co*-OEGMEMA) film-coated PET was thoroughly washed with pure water to remove any physisorbed polymers, and then dried in a stream of argon. The copolymer film-coated substrate was immersed into an ethanolic solution of biotin-TEG-NH_2 (0.1 mg/mL) for 1 h at room temperature, before the resulting substrate was washed with ethanol and pure water, and then dried in a stream of argon.

2.4. Generation of protein pattern on copolymer film-coated PET substrates

Polydimethylsiloxane (PDMS) stamps were prepared, according to the literature method.[34] Briefly, a micropatterned silicon wafer used as a master was developed with a negative photoresist (SU8-50, MicroChem) and photolithography technique. Following this, the master was coated with (tridecafluoro-1,1,2,2-tetrahydrooctyl)trichlorosilane under a vacuum for 2 h. To cast the PDMS stamp, the master was placed in a petri dish and covered with PDMS oligomers. After curing for 6 h at 60 °C, the PDMS stamp was peeled off, cleaned, and oxidized using the oxygen plasma cleaner for 1 min at medium strength. The patterned-PDMS stamp (50 μm lateral lines separated by 100 μm) was inked with the PBS buffer solution of biotin-TEG-NH_2 (0.1 mg/mL) using the spin-coater. The inked stamp was brought into contact with the poly(NAS-*co*-OEGMEMA) film-coated PET for 60 s. The stamp was carefully peeled off, and the biotin-patterned substrate was immersed in the buffer solution of rhodamine-labeled streptavidin (1 mg/mL) for 30 min at room temperature. The protein patterned image was obtained using a confocal microscope (LSM 700 META, Carl Zeiss) after the sample was washed several times with the buffer solution and distilled water, and then dried in a stream of argon.

2.5. Cell culture and cytotoxicity test

HeLa cells were cultured as adherent cells in DMEM (Dulbecco's modified eagle medium, Invitrogen, custom order). The DMEM was supplemented with 10% fetal bovine serum dialyzed with a cut-off of 10 kDa (Invitrogen, 26400-044), 100 U/mL penicillin/streptomycin, 4 mM L-Glutamine. Cells were plated at a density of 150 cells/mm^2.

2.6. Characterizations

2.6.1. Contact angle goniometry

Static contact angle of a pure water droplet (approximately, 5 μL in volume) was measured by Phoenix 300 apparatus (Surface Electro Optics Co. Ltd., Gyunggido, South Korea) equipped with a video camera. Reported values represented the averages of at least 3 independent measurements.

2.6.2. X-ray Photoelectron spectroscopy (XPS)

XPS analysis was performed using a VG Scientific ESCALAB 250 spectrometer (UK) with a monochromatic Al Kα X-ray source. A multichannel detector was used to measure emitted photoelectrons at a take-off angle of 90° relative to the surface. During the process, the base pressure was 10^{-9}-10^{-10} Torr. Survey and high-resolution spectra were obtained at a resolution of 1 eV from three scans and of 0.05 eV from 5 to 20 scans, respectively. All binding energies were determined with the C 1s peak at 284.6 eV as a reference.

2.6.3. Scanning probe microscopy (SPM)

SPM experiments were carried out using an NX20 (Park Systems Co., Suwon, South Korea) in a non-contact mode (tip type: PPP-NCHR) at a scan rate of 1.0 Hz.

2.6.4. Field-emission scanning electron microscopy (FE-SEM)

All samples were fractured with two tweezers in liquid nitrogen at room temperature. The fractured samples were platinum/palladium (thickness: 1.6 nm) coated in an ion sputter (Hitachi E-1010, Japan). The SEM images were obtained using a Hitachi S-4800 with a magnification of ×70 k (accelerating voltage: 3 kV). (e) Phase contrast microscopy. Phase contrast microscopy was conducted under an inverted microscope (IX71, Olympus, Japan) equipped with a CCD microscope camera (DP71, Olympus).

3. Results and discussion

Poly(NAS-*co*-OEGMEMA) film was chosen as a coating polymer for fabricating PET substrates as it does not necessary an activation process for immobilizing bioactive ligands, owing to its intrinsically activated functional group (*i.e.,* succinimidyl ester).[32] Furthermore, the biotin-terminated, poly(NAS-*co*-OEGMEMA) film displayed low biofouling levels against non-target proteins as well as a high signal-to-noise ratio (SNR) to the target protein (*i.e.,* streptavidin) without employing a backfilling process. Figure 1 showed a general procedure for the synthesis of a biotinylated, poly(NAS-*co*-OEGMEMA) film on PET substrates. Briefly, an initiator (**1**) was spin-coated on an oxidized PET substrate, and the sample was then baked at 60 °C for 20 min, followed by UV exposure for 1 h at room temperature. The initiator-anchored substrate was washed, and SI-ARGET ATRP was carried out with NAS (0.2 mmol) and OEGMEMA (0.8 mmol) to graft the activation-free, bioactive poly(NAS-*co*-OEGMEMA) film on PET surfaces. Biotin-TEG-NH_2 (**4**) was immobilized on the copolymer film using an amide coupling reaction, producing in a biotin-terminated, poly(NAS-*co*-OEGMEMA) film-coated PET surface (Figure 1).

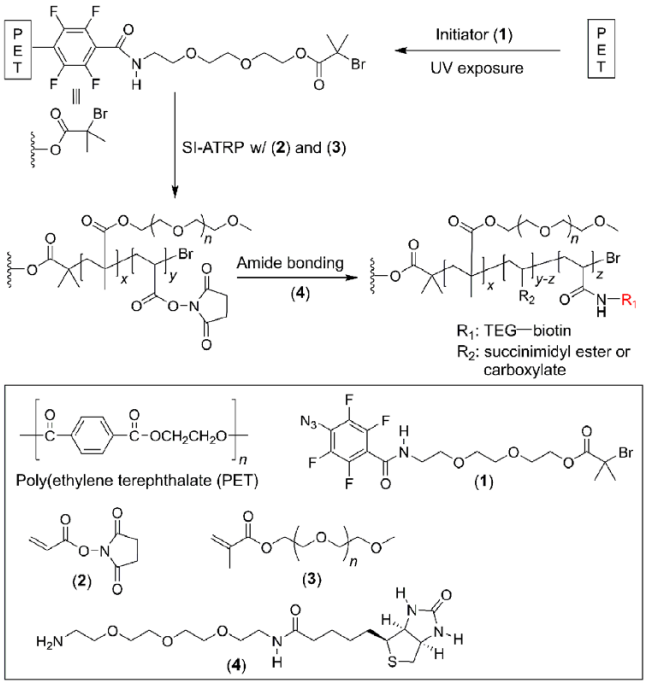

Figure 1. Schematic procedure of the formation of a biotinylated, poly(NAS-*co*-OEGMEMA) film on PET.

We characterized the PET surface after each step by contact angle goniometry, X-ray photoelectron spectroscopy (XPS), scanning probe microscopy (SPM), and field-emission scanning electron microscopy (FE-SEM). Figure 2 showed the graph and image on static contact angle of pure water after each process. After plasma cleaning of the bare PET, the contact angle changed to < 5° from 76° (Figure 2(b)-(c)), which indicated the generation of oxygen-bearing functional groups including alcohol, epoxide, ketone, and carboxylic acid.[29,30,35] Subsequently, immobilizing initiator (**1**) onto the PET surface increased the water contact angle to 16° (Figure 2(d)). The initiator-immobilized PET was further confirmed by SI-ARGET ATRP with NAS and OEGMEMA; the contact angle was measured with 40° for the copolymer film after the washing process (Figure 2(e)). We assume that succinimidyl ester groups of the copolymer film make it more hydrophobic than that of initiator-anchored PET surfaces. After biotinylation, the contact angle was similar with that of the copolymer film, and this result suggested that the biotin group did not considerably change the contact angle of the copolymer film.

XPS analysis confirmed the successful functionalization of the PET surface at each step as shown in Figure 3. In the wide-scan XPS spectra, the O 1s and C 1s peaks of intact PET substrate were observed at 532 and 285 eV, respectively (Figure 3(a)). After immobilizing of initiator (**1**), the characteristic peaks of (**1**) were sharply detected at 686.8 (F 1s), 399.3 (N 1s), 183.0 (Br 3p), and 69.7 eV (Br 3d). These results indicated that the initiator (**1**), consisting of the perfluorophenyl ring and ATRP initiator moiety, was successfully anchored on the intact PET substrate (Figure 3(b)). The formation of copolymer film on PET decreased the peak intensities of F 1s, Br 3d, and Br 3p,

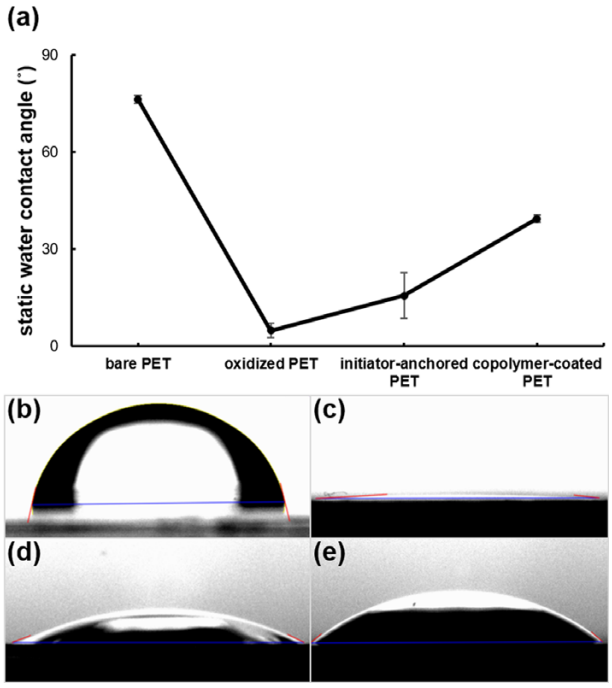

Figure 2. Static water contact angle measurement of (a) summary, (b) intact PET, (c) plasma-cleaned PET, (d) initiator-anchored PET, and (e) poly(NAS-*co*-OEGMEMA) film-coated PET.

and increased the peak intensity of C 1s. The peak of N 1s in the succinimidyl ester group weakly appeared at 400.6 eV (Figure 3(c)). After biotinylation, the peak intensity of N 1s was increased slightly. To further support, we also analyzed the XPS high-resolution scan of the N 1s peaks at each step. The amide group of the initiator (**1**) was observed at 398.7 eV (Figure 3(e)), and a new peak appeared at 400.5 eV, originated from succinimidyl ester (Figure 3(f)); the difference of binding energy was approximately 1.8 eV, which was consistent with the previously obtained value.[36,37] The peaks of N 1s in the biotinylated, copolymer film on PET were deconvoluted at 401.4, 399.5, and 398.5 eV, respectively. We assigned the peaks based on the literature:[38] the ureido moiety (401.1 eV), the amide group of biotin ligand in the copolymer film (399.5 eV), and the amide groups of ATRP initiator (398.5 eV) (Figure 3(g)).

In addition, we monitored surface morphology before and after the fabrication of PET substrate using scanning probe microscopy (SPM) and field-emission scanning electron microscopy (FE-SEM). In SPM height images obtained in non-contact mode, the copolymer-coated PET exhibited a smooth surface, compared with the oxidized surface and the initiator-anchored surface (Figure 4(a)-(c)). As a result, root-mean-square (RMS) roughness of the whole surface area was 3.43 nm for the plasma-cleaned

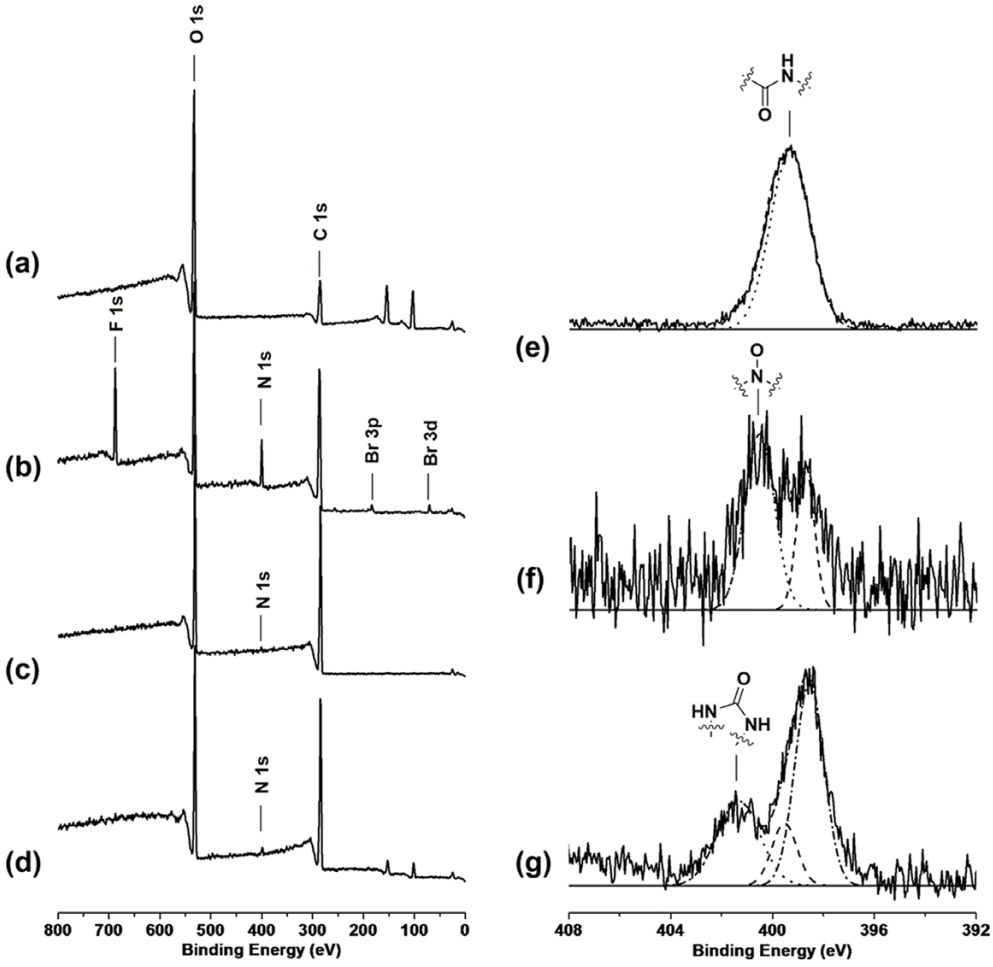

Figure 3. XPS survey-scan spectra of (a) intact PET, (b) initiator-anchored PET, (c) poly(NAS-*co*-OEGMEMA) film-coated PET, and (d) biotinylated, poly(NAS-*co*-OEGMEMA) film-coated PET. XPS high-resolution spectra of N 1s in (e) initiator-anchored PET, (f) poly(NAS-*co*-OEGMEMA) film-coated PET, and (g) biotinylated, poly(NAS-*co*-OEGMEMA) film-coated PET.

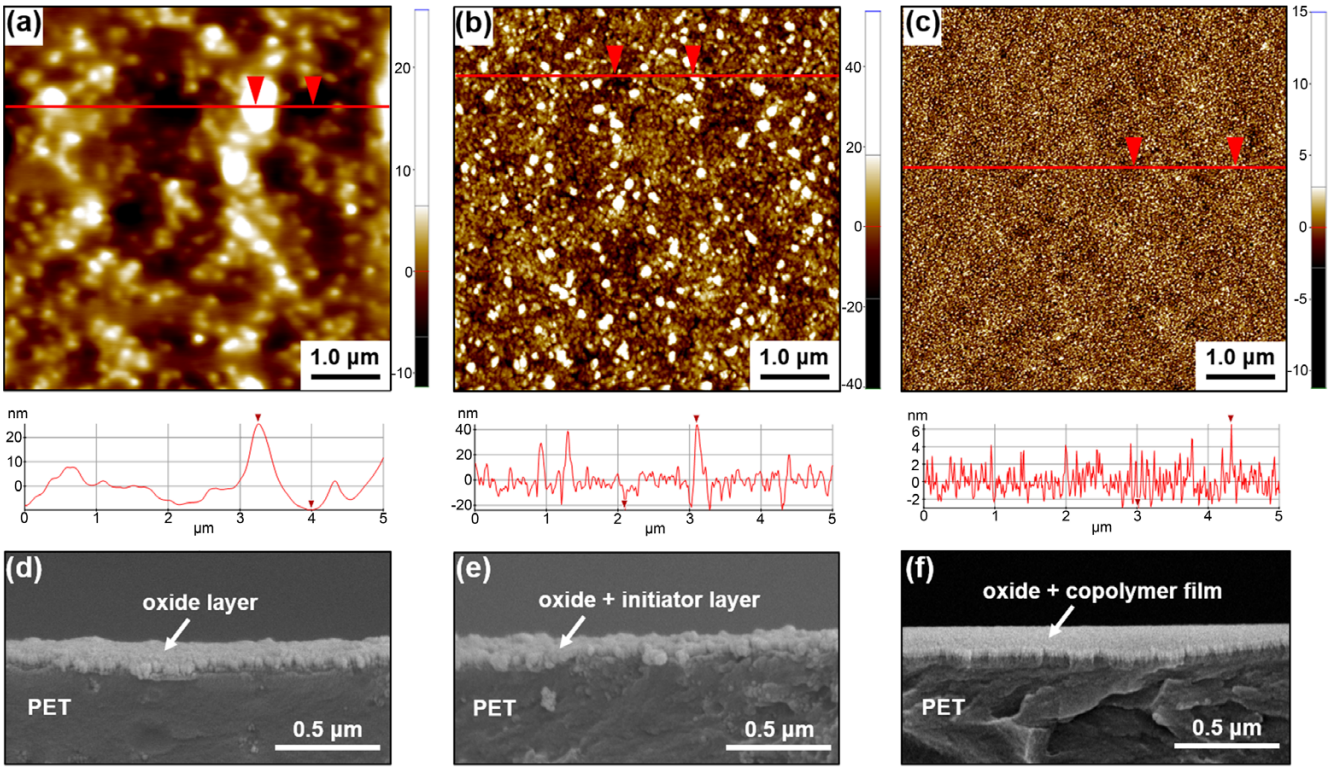

Figure 4. SPM images of (a) plasma-cleaned PET, (b) initiator-anchored PET, and (c) poly(NAS-*co*-OEGMEMA) film-coated PET; The red line is indicative of the line roughness profile. FE-SEM images of (d) plasma-cleaned PET, (e) initiator-anchored PET, and (f) poly(NAS-*co*-OEGMEMA) film-coated PET.

PET, 9.23 nm for the initiator-anchored PET, and 1.44 nm for copolymer-coated PET. The line profile, which was indicative of surface roughness along the red line in the image, also represented the smoothness of each PET surface as shown below each SPM image. The RMS line roughness was 7.1 nm for the oxidized PET (maximum height difference: 35 nm), 9.8 nm for the initiator-anchored PET (maximum height difference: 65 nm), and 1.5 nm for the copolymer-coated PET (maximum height difference: 9 nm). The cross-section FE-SEM image corresponded with the SPM image at each step (Figure 4(d)-(f)). After polymerization, the copolymer film-coated PET surface was considerably flatter than the oxidized and the initiator-anchored PET surfaces. Because of the uniform growth rate of the polymer chain *via* SI-CRP, the overall surface morphology of the polymer film on the surface was fairly smooth.[39] Huck research group and we also demonstrated that the surface roughness was affected by the anchored initiator density on the surface.[40,41] Thus, we assume that the flatter copolymer film surface, obtained in this work, resulted from the closely packed monolayer of the initiator, anchored on the PET surface.

We evaluated the functionality and non-biofouling performances of the biotinylated, copolymer film-coated PET surface using protein patterning. Figure 5(a) depicted the process of the protein patterning on the copolymer film-coated PET surface. The biotin-patterned copolymer film was generated using a microcontact printing technique based on a PDMS stamp. The stamp having relief features of 50 μm lateral lines separated by 100 μm had been inked with biotin-TEG-NH_2 (1 mg/mL in ethanol). The inked stamp was in conformal contact with the

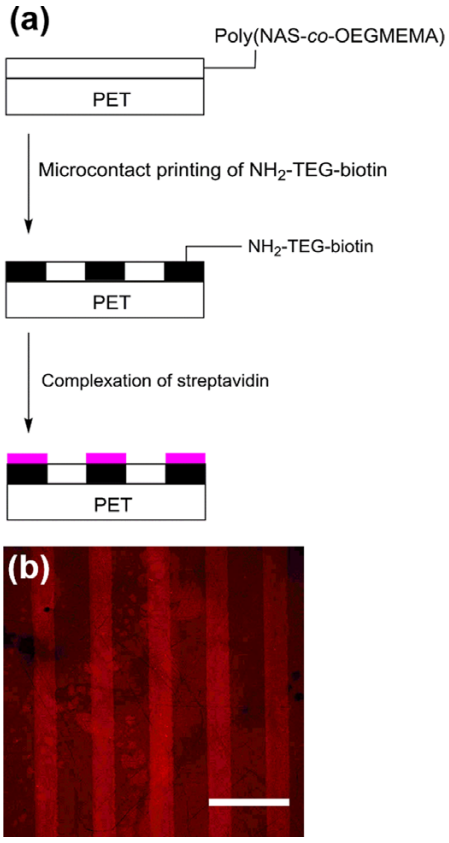

Figure 5. (a) Schematic procedure of the generating protein pattern and (b) confocal laser scanning microscopy image of rhodamine-conjugated streptavidin on the biotin-patterned poly(NAS-*co*-OEGMEMA) film-coated PET. The scale bar is 200 μm.

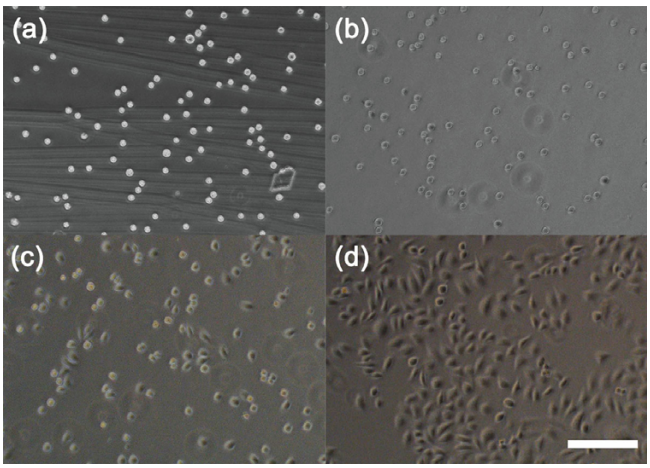

Figure 6. Phase contrast images of HeLa cells observed on PLL-treated, copolymer film-coated PET at (a) 0 h, (b) 1 h, (c) 6 h, and (d) 25 h after plating. The scale bar is 100 μm.

copolymer film for 1 min, and the resulting substrate was carefully washed with ethanol and the PBS buffer solution. Without employing a passivation step, the biotinylated, patterned substrate was incubated in the buffer solution of rhodamine-labeled streptavidin (0.1 mg/mL) for 2 h at room temperature. After washing with the buffer solution, the protein-patterned copolymer film was characterized by confocal laser scanning microscopy (Figure 5(b)). The red vertical lines resulting from the dye-labeled streptavidin were contrasted with the background. The SNR [(average signal intensity–average background intensity)/standard deviation of background intensity] was approximately 4.7. Consequently, we confirmed the coating of non-biofouling poly(NAS-*co*-OEGMEMA) films on a PET surface and successfully generated a protein-patterned copolymer film using a soft lithography technique. In addition to the protein patterning, the biocompatibility of copolymer film-coated PET was evaluated with HeLa cells. The copolymer-coated PET was conjugated with poly-L-lysine, and HeLa cells were plated with a density of 150 cells/mm^2. Figure 6 showed that the cells adhered, spread, grew, and proliferated normally on the film, which indicated that the PET film itself, and the polymer grown on top of it did not have negative effects on cellular growth.

4. Conclusions

In summary, we have functionalized PET surfaces using a perfluoroaryl azide-based photochemical reaction, and subsequently synthesized a functionalized, non-biofouling copolymer film on the substrate through SI-CRP with NAS and OEGMEMA. This copolymer system made it easy to generate a protein pattern on the PET surface assisted using a microcontact printing technique with neither post functionalization or passivation process. Owing to its reproducibility and versatility, we believe that this strategy, employed in this work, will improve biocompatibility and bioactivity of PET substrate, and widen the applications of organic polymer substrates; thus, these materials can be used in human implantation.

References

(1) U. K. Thiele, *Polyester Bottle Resins, Production, Processing, Properties and Recycling*, Heidelberg Business Media, Heidelberg, 2007, p 85.
(2) V. B. Gupta and Z. Bashir, *Handbook of Thermoplasitc Polyesters,* Wiley-VCH, Weinheim, 2002.
(3) H. Köpnick, M. Schmidt, W. Brügging, J. Rüter, and W. Kaminsky, *Polyesters in Ulmann's Encyclopedia of Industrial Chemistry,* Wiley-VCH, Weinheim, 2005, pp 233-238.
(4) K. Ohno, Y. Kayama, V. Ladmiral, T. Fukuda, and Y. Tsujii, *Macromolecules*, **43**, 5569 (2010).
(5) C. C. Ibeh, *Thermoplactic Materials: Properties, Manufacturing Methods, and Applications*, CRC Press, Boca Raton, Florida, 2011.
(6) J. W. Leem, M. Choi, and J. S. Yu, *ACS Appl. Mater. Interfaces,* **7**, 2349 (2015).
(7) W. Gutowski, H. Dodiuk, and K. L. Mittal, *Recent Advances in Adhesion Science and Technology: In Honor of Dr. Kash Mittal*, CRC Press, Boca Raton, Florida, 2013.
(8) J. E. Puskas and Y. H. Chen, *Biomacromolecules,* **5**, 1141 (2004).
(9) A. Metzger, *Biomed. Eng.,* **11**, 301 (1976).
(10) L. Barbe, B. Boval, M. P. Wautier, and J. L. Wautier, *Transfusion,* **40**, 1250 (2000).
(11) N. Angelova and D. Hunkeler, *Trends Biotechnol.,* **17**, 409 (1999).
(12) A. J. Domb and W. Khan, in *Advances in Delivery Science and Technology*, Springer, New York, 2014.
(13) N. Blanchemain, S. Haulon, B. Martel, M. Traisnel, M. Morcellet, and H. F. Hildebrand, *Eur. J. Vasc. Endovasc.,* **29**, 628 (2005).
(14) T. Ueberrueck, J. Tautenhahn, L. Meyer, O. Kaufmann, H. Lippert, I. Gastinger, and T. Wahlers, *J. Surg. Res.,* **124**, 305 (2005).
(15) N. Blanchemain, S. Haulon, F. Boschin, E. Marcon-Bachari, M. Traisnel, M. Morcellet, H. F. Hildebrand, and B. Martel, *Biomol. Eng.,* **24**, 149 (2007).
(16) P. A. Ramires, L. Mirenghi, A. R. Romano, F. Palumbo, and G. Nicolardi, *J. Biomed. Mater. Res.,* **51**, 535 (2000).
(17) N. Poddevin, M. W. King, and R. G. Guidoin, *J. Biomed. Mater. Res.,* **38**, 370 (1997).
(18) N. Poddevin, B. Cronier, Y. Marois, J. P. Delagoutte, D. Mainard, J. H. Jaeger, A. Y. Belanger, M. W. King, and R. Guidoin, *Rev. Chir. Orthop. Reparatrice Appar. Mot.,* **81**, 410 (1995).
(19) W. K. Cho, S. M. Kang, and J. K. Lee, *J. Nanosci. Nanotechnol.,* **14**, 1231 (2014).
(20) B. S. Lee, J. Lee, G. Han, E. Ha, I. S. Choi, and J. K. Lee, *Chem. Asian J.,* **11**, 2057 (2016).
(21) B. S. Lee, Y. S. Chi, K. B. Lee, Y. G. Kim, and I. S. Choi, *Biomacromolecules,* **8**, 3922 (2007).
(22) I. Banerjee, R. C. Pangule, and R. S. Kane, *Adv. Mater.,* **23**, 690 (2011).
(23) S. Roux and S. Demoustier-Champagne, *J. Polym. Sci., Part A: Polym. Chem.,* **41**, 1347 (2003).
(24) T. Farhan and W. T. S. Huck, *Eur. Polym. J.,* **40**, 1599 (2004).
(25) K. Fukazawa, A. Nakao, M. Maeda, and K. Ishihara, *Acs. Appl. Mater. Inter.,* **8**, 24994 (2016).
(26) J. Kim, D. Hong, S. Jeong, B. Kong, S. M. Kang, Y. G. Kim, and I. S. Choi, *Chem. Asian J.,* **6**, 363 (2011).
(27) S. P. Jeong, D. Hong, S. M. Kang, I. S. Choi, and J. K. Lee, *Asian J. Org. Chem.,* **2**, 568 (2013).
(28) S. P. Jeong, S. M. Kang, D. Hong, H. Y. Lee, I. S. Choi, S. Ko, and J. K. Lee, *J. Nanosci. Nanotechnol.,* **15**, 1767 (2015).
(29) J. Raj, G. Herzog, M. Manning, C. Volcke, B. D. MacCraith, S. Ballantyne, M. Thompson, and D. W. M. Arrigan, *Biosens. Bioelectron.,* **24**, 2654 (2009).
(30) S. Laib and B. D. MacCraith, *Anal. Chem.,* **79**, 6264 (2007).
(31) J. Zhang, C. Das, and Z. H. Fan, *Microfluid. Nanofluid.,* **5**, 327 (2008).
(32) B. S. Lee, H. Kim, I. S. Choi, and W. K. Cho, *J. Polym. Sci., Part A: Polym.*

Chem., **55**, 329 (2017).
(33) M. D. Yan, S. X. Cai, M. N. Wybourne, and J. F. W. Keana, *J. Am. Chem. Soc.,* **115**, 814 (1993).
(34) K. B. Lee, Y. Kim, and I. S. Choi, *Bull. Korean Chem. Soc.,* **24**, 161 (2003).
(35) A. Larsson, T. Ekblad, O. Andersson, and B. Liedberg, *Biomacromolecules,* **8**, 287 (2007).
(36) B. S. Lee, S. Park, K. B. Lee, S. Jon, and I. S. Choi, *Biointerphases,* **2**, 136 (2007).
(37) T. Bocking, K. A. Kilian, T. Hanley, S. Ilyas, K. Gaus, M. Gal, and J. J. Gooding, *Langmuir,* **21**, 10522 (2005).
(38) W. J. Gammon, O. Kraft, A. C. Reilly, and B. C. Holloway, *Carbon,* **41**, 1917 (2003).
(39) R. Barbey, L. Lavanant, D. Paripovic, N. Schuwer, C. Sugnaux, S. Tugulu, and H. A. Klok, *Chem. Rev.,* **109**, 5437 (2009).
(40) D. M. Jones, A. A. Brown, and W. T. S. Huck, *Langmuir,* **18**, 1265 (2002).
(41) S. P. Jeong, B. S. Lee, S. M. Kang, S. Ko, I. S. Choi, and J. K. Lee, *Chem. Commun.,* **50**, 5291 (2014).

